

## Analytical solutions to piezoelectric bimorphs based on improved FSDT beam model

Yan-guo Zhou<sup>†</sup>, Yun-min Chen<sup>‡</sup> and Hao-jiang Ding<sup>‡†</sup>

Department of Civil Engineering, Zhejiang University, Hangzhou 310027, P. R. China

(Received April 8 2005, Accepted July 25 2005)

**Abstract.** This paper presents an efficient and accurate coupled beam model for piezoelectric bimorphs based on improved first-order shear deformation theory (FSDT). The model combines the equivalent single layer approach for the mechanical displacements and a layerwise modeling for the electric potential. General electric field function is proposed to reasonably approximate the through-the-thickness distribution of the applied and induced electric potentials. Layerwise defined shear correction factor ( $k$ ) accounting for nonlinear shear strain distribution is introduced into both the shear stress resultant and the electric displacement integration. Analytical solutions for free vibrations and forced response under electromechanical loads are obtained for the simply supported piezoelectric bimorphs with series or parallel arrangement, and the numerical results for various length-to-thickness ratios are compared with the exact two-dimensional piezoelectricity solution. Excellent predictions with low error estimates of local and global responses as well as the modal frequencies are observed.

**Keywords:** piezoelectric bimorph; beam model; first-order shear deformation theory; shear correction factor; electric potential; analytical solution

---

### 1. Introduction

Piezoelectric bimorphs (or benders) are a special type of smart structures, and have been widely used as sensors or actuators in many applications due to the characteristics of miniaturization, high positioning accuracy, sensitive response, and large displacement (Ha and Kim 2002, Zhou, *et al.* 2005). A bimorph consists of two identical piezoelectric elements stacked on top of each other (parallel or series arrangement), and the application of an electric field across the two layers of the bimorph produces one layer to expand while the other one contracts, which results in a bending deformation. This is the working principle of bimorphs. More sophisticated multilayer piezoelectric composites were developed from bimorphs to improve the motion amplification and performance of the smart structures (Steel, *et al.* 1978). Thus, for the design and application of such bimorphs, it is crucial to accurately model their electromechanical behaviors.

The analysis of piezoelectric composite structures like bimorphs requires efficient and accurate modeling of both the mechanical and electric responses, and in the past decades the study in this field

---

<sup>†</sup>Ph.D. Candidate, E-mail: qzking@zju.edu.cn

<sup>‡</sup>Professor, Corresponding Author, E-mail: cym@civil.zju.edu.cn

<sup>‡†</sup>Professor, E-mail: hjding@mail.hz.zj.cn

has experienced tremendous growth (Rao and Sunar 1994, Chee, *et al.* 1998, Saravanos and Heyliger 1999). Although some three-dimensional (3D) analytical solutions have been presented with exact satisfactions for the piezoelectric structures (Tzou and Tiersten 1994, Lee and Jiang 1996, He, *et al.* 2000, Lim, *et al.* 2001), they are available only for some regular shapes with specified simple boundary conditions. And the corresponding finite element implementation typically requires high computational effort and becomes intractable especially for dynamics and control problems (Hwang and Park 1993, Wang 2004). Thus the introduction of simpler and more practical 2D (1D for beams) analytical models is desirable for the possible solution to more general piezoelectric composite structures (Smits, *et al.* 1991, Kapuria 2001).

The present work attempts to develop consistent, yet comprehensive FSDT beam model (Gopinathan, *et al.* 2000) for piezoelectric bimorphs. This model combines an equivalent single layer (ESL) approach for the mechanical displacements with a layerwise approximation for the electric potential so as to achieve the accuracy of layerwise method while preserving the computational advantage of ESL theory for the mechanical field variables. For the electric potential in piezoelectric layers, besides the linear distribution assumptions along the thickness direction for the surface-applied electric potential, quadratic functions are adopted to approximate the strain-induced electric potential. The differential equations of motion are solved analytically for series and parallel arrangements, with particular attention devoted to the boundary conditions on the outer faces and the interface continuity conditions. Numerical results for the simply supported bimorphs under flexural deformation conditions are presented for various length-to-thickness ratios, and the results are verified by those obtained from the exact 2D model via state space approach (Ding, *et al.* 2000, Tarn 2002).

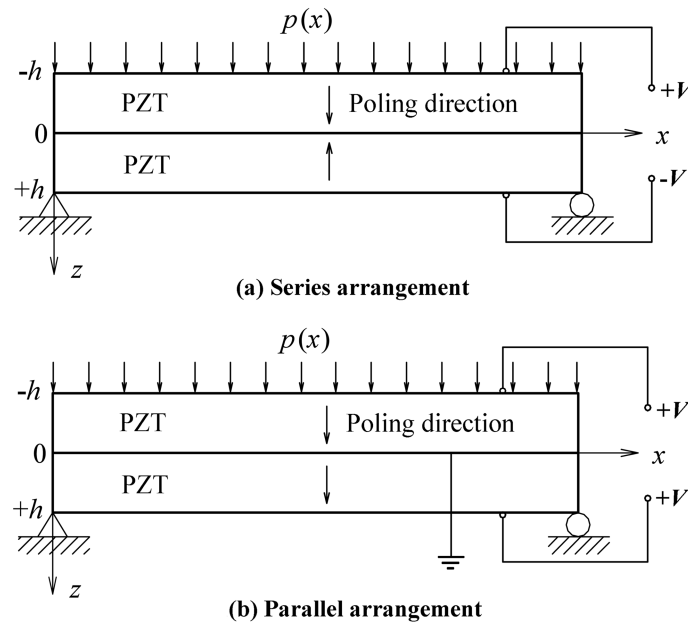


Fig. 1 Typical piezoelectric bimorph settings

## 2. Beam model and field approximations

Fig. 1 shows the geometry and typical settings of bimorphs. For either type of arrangement, the bimorph of unit width comprises two identical piezoelectric layers with a length of  $l$ , and the thickness of the each piezoelectric layer is  $h$ . Two layers are considered perfectly bonded. Hence, the mechanical displacements and transverse stresses, and electric potential have to be continuous through the bimorph interfaces. In view of the fact that generally the width is relatively short than the length, piezoelectric bimorphs can be treated as a symmetric plane stress beam. The bimorph may undergo the external mechanical and electric loads (e.g. a distributed surface load,  $p(x, t)$ , and an applied electric voltage,  $V(x, t)$ ) under isothermal conditions, and is assumed to deflect in the  $x$ - $z$  plane only.

### 2.1. Basic equations of piezoelectricity and beam equations

The linear field equations of motion for two-dimensional orthotropic piezoelectricity are given by (Sosa and Castro 1993, Ding, *et al.* 1997)

$$\frac{\partial \sigma_x}{\partial x} + \frac{\partial \tau_{xz}}{\partial z} + f_x = \rho \frac{\partial^2 u_x}{\partial t^2}, \quad \frac{\partial \tau_{xz}}{\partial x} + \frac{\partial \sigma_z}{\partial z} + f_z = \rho \frac{\partial^2 u_z}{\partial t^2}, \quad \frac{\partial D_x}{\partial x} + \frac{\partial D_z}{\partial z} = 0 \quad (1)$$

where  $\rho$  is the mass density of piezoelectric material;  $u_x$  and  $u_z$  are the displacement components of the bimorph in the longitudinal and transverse directions respectively;  $f_x$  and  $f_z$  are the body forces;  $\sigma_x$ ,  $\sigma_z$ ,  $\tau_{xz}$ ,  $D_x$  and  $D_z$  represent the stress components, electric displacement components, and they satisfy the linear constitutive equations of piezoelectricity under 2D plane assumptions as following:

$$\sigma_x = \bar{c}_{11}\varepsilon_x + \bar{c}_{13}\varepsilon_z - (-1)^i \bar{e}_{31}E_z, \quad \sigma_z = \bar{c}_{13}\varepsilon_x + \bar{c}_{33}\varepsilon_z - (-1)^i \bar{e}_{33}E_z \quad (2a)$$

$$\tau_{xz} = c_{55}\gamma_{xz} - (-1)^i e_{15}E_x, \quad D_z = (-1)^i (\bar{e}_{31}\varepsilon_x + \bar{e}_{33}\varepsilon_z) + \bar{e}_{33}E_z, \quad D_x = (-1)^i e_{15}\gamma_{xz} + \varepsilon_{11}E_x \quad (2b)$$

where  $i$  is an integer and  $i=2$  if the layer poling direction coincides with the coordinate axes and otherwise  $i=1$ ;  $\varepsilon_x$ ,  $\varepsilon_z$ ,  $\gamma_{xz}$ ,  $E_x$  and  $E_z$  are strain and electric field intensity components, which relate to the displacement components and electric potential  $\phi$  by

$$\varepsilon_x = \frac{\partial u_x}{\partial x}, \quad \varepsilon_z = \frac{\partial u_z}{\partial z}, \quad \gamma_{xz} = \frac{\partial u_x}{\partial z} + \frac{\partial u_z}{\partial x}, \quad E_x = -\frac{\partial \phi}{\partial x}, \quad E_z = -\frac{\partial \phi}{\partial z} \quad (3)$$

It should be noted that  $\bar{c}_{11}$ ,  $\bar{c}_{13}$ ,  $\bar{c}_{33}$ ,  $\bar{e}_{31}$ ,  $\bar{e}_{33}$  and  $\bar{e}_{33}$  in Eq. (2) are the reduced material constants of the piezoelectric medium under plane stress assumption from 3D constitutive relationship:

$$\bar{c}_{11} = c_{11} - \frac{c_{12}^2}{c_{22}}, \quad \bar{c}_{13} = c_{13} - \frac{c_{12}c_{23}}{c_{22}}, \quad \bar{c}_{33} = c_{33} - \frac{c_{23}^2}{c_{22}}$$

$$\bar{e}_{31} = e_{31} - \frac{c_{12}c_{32}}{c_{22}}, \quad \bar{e}_{33} = e_{33} - \frac{c_{23}e_{32}}{c_{22}}, \quad \bar{e}_{33} = e_{33} + \frac{e_{32}^2}{c_{22}} \quad (4)$$

For a beam with small width, introduce the zero normal stress assumption, namely,  $\sigma_z$  is negligible compared with other stress components. Substituting  $\sigma_z=0$  into Eq. (1) yields

$$\frac{\partial \sigma_x}{\partial x} + \frac{\partial \tau_{xz}}{\partial z} + f_x = \rho \frac{\partial^2 u_x}{\partial t^2}, \quad \frac{\partial \tau_{xz}}{\partial x} + f_z = \rho \frac{\partial^2 u_z}{\partial t^2}, \quad \frac{\partial D_x}{\partial x} + \frac{\partial D_z}{\partial z} = 0 \quad (5)$$

And solving  $\sigma_z=0$  in Eq. (2a) for  $\varepsilon_z$  gives

$$\varepsilon_z = -\frac{\bar{c}_{13}}{\bar{c}_{33}}\varepsilon_x + (-1)^i \frac{\bar{e}_{33}}{\bar{c}_{33}}E_z \quad (6)$$

On use of Eq. (6), the 2D constitutive relations in Eqs. (2) reduce to

$$\sigma_x = \left(\bar{c}_{11} - \frac{\bar{c}_{13}^2}{\bar{c}_{33}}\right)\varepsilon_x - (-1)^i \left(\bar{e}_{31} - \frac{\bar{c}_{13}\bar{e}_{33}}{\bar{c}_{33}}\right)E_z, \quad \tau_{xz} = c_{55}\gamma_{xz} - (-1)^i e_{15}E_x \quad (7a)$$

$$D_z = (-1)^i \left(\bar{e}_{31} - \frac{\bar{c}_{13}\bar{e}_{33}}{\bar{c}_{33}}\right)\varepsilon_x + \left(\bar{e}_{33} + \frac{\bar{e}_{33}^2}{\bar{c}_{33}}\right)E_z, \quad D_x = (-1)^i e_{15}\gamma_{xz} + \varepsilon_{11}E_x \quad (7b)$$

And the needed general strain-displacement relations in Eq. (3) reduce to

$$\varepsilon_x = \frac{\partial u_x}{\partial x}, \quad \gamma_{xz} = \frac{\partial u_x}{\partial z} + \frac{\partial u_z}{\partial x}, \quad E_x = -\frac{\partial \phi}{\partial x}, \quad E_z = -\frac{\partial \phi}{\partial z} \quad (8)$$

## 2.2. Mechanical displacement and electric potential approximations

According to first-order shear deformation theory, when thick beams are considered, the effect of shear deformation (and rotary inertia in dynamic analysis) cannot be omitted. It is assumed that (See Fig. 2): 1) Straight material lines that are perpendicular to the neutral axis in the undeformed state remain straight in the deformed state even though they may not remain perpendicular to the neutral axis; 2) The compression in a direction normal to the neutral axis of the beam is negligible (i.e. no ‘‘thickness stretch’’) and the transverse displacement,  $w$ , keeps constant through the cross section.

The FSDT approximation is thus assumed for the mechanical displacements as follows:

$$u_z(x, z, t) = w(x, t), \quad u_x(x, z, t) = -z\psi(x, t) \quad (9)$$

where  $w$  is the displacement of the neutral axis of the bimorph; and  $\psi$  is the bending rotations of vertical lines perpendicular to the neutral axis.

Using Eqs. (8) and (9), we get the strain of the piezoelectric layer given by

$$\varepsilon_x = -z\frac{\partial \psi}{\partial x}, \quad \gamma_{xz} = -\psi + \frac{\partial w}{\partial x} \quad (10)$$

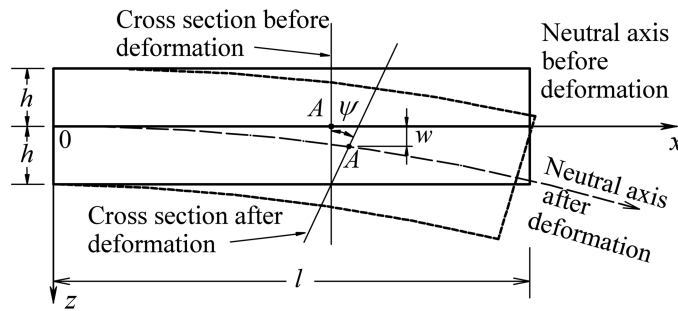


Fig. 2 Piezoelectric bimorph: coordinates and geometry

The electric potential can be generally associated with the applied electric potential on the bimorph faces or at the layer interface, and with the induced electric potential by elastic deformation in the piezoelectric layer. Consequently, we propose the following functions

$$\phi(x, z, t) = g(z)V(x, t) + f(z)\Phi(x, t) \quad (11)$$

where  $V(x, t)$  is the amplitude at surfaces of the applied electric potential, and  $g(z)$  is the through-the-thickness distribution function of this applied electric potential, which is well acknowledged as a linear distribution (Smits, *et al.* 1991);  $\Phi(x, t)$  is the amplitude of induced electric potential on the midline of each piezoelectric layer, and  $f(z)$  is the through-the-thickness distribution function, which can be approximated in various models in the literature (Wang and Quek 2000).

Therefore, the electric potential distribution functions in Eq. (11) can be approximated as

$$g(z) = \begin{cases} (-1)^i \left(\frac{-z}{h}\right), & -h \leq z \leq 0 \\ (-1)^i \left(\frac{z}{h}\right), & 0 \leq z \leq h \end{cases}, \quad f(z) = \begin{cases} (-1)^i \left[1 - \left(\frac{z+h/2}{h/2}\right)^2\right], & -h \leq z \leq 0 \\ (-1)^i \left[1 - \left(\frac{z-h/2}{h/2}\right)^2\right], & 0 \leq z \leq h \end{cases} \quad (12)$$

Substituting the above assumed  $\phi(x, z, t)$  into Eq. (8), one may obtain the electric field intensity components, then substituting this results and Eq. (10) into Eq. (7) yields the coupled electromechanical variables for either type of arrangement given by

$$\sigma_x = \begin{cases} -\left(\bar{c}_{11} - \frac{\bar{c}_{13}^2}{\bar{c}_{33}}\right)z \frac{\partial \psi}{\partial x} - \left(\bar{e}_{31} - \frac{\bar{c}_{13}}{\bar{c}_{33}} \bar{e}_{33}\right) \left[8 \frac{z+h/2}{h^2} \Phi + \frac{1}{h} V\right], & -h \leq z \leq 0 \\ -\left(\bar{c}_{11} - \frac{\bar{c}_{13}^2}{\bar{c}_{33}}\right)z \frac{\partial \psi}{\partial x} - \left(\bar{e}_{31} - \frac{\bar{c}_{13}}{\bar{c}_{33}} \bar{e}_{33}\right) \left[8 \frac{z-h/2}{h^2} \Phi - \frac{1}{h} V\right], & 0 \leq z \leq h \end{cases} \quad (13a)$$

$$\tau_{xz} = \begin{cases} c_{55} \left(-\psi + \frac{\partial w}{\partial x}\right) - e_{15} \left\{ \left[1 - \left(\frac{z+h/2}{h/2}\right)^2\right] \frac{\partial \Phi}{\partial x} + \frac{z}{h} \frac{\partial V}{\partial x} \right\}, & -h \leq z \leq 0 \\ c_{55} \left(-\psi + \frac{\partial w}{\partial x}\right) - e_{15} \left\{ \left[1 - \left(\frac{z-h/2}{h/2}\right)^2\right] \frac{\partial \Phi}{\partial x} - \frac{z}{h} \frac{\partial V}{\partial x} \right\}, & 0 \leq z \leq h \end{cases} \quad (13b)$$

$$D_x = \begin{cases} (-1)^i \left\{ e_{15} \left(-\psi + \frac{\partial w}{\partial x}\right) + \epsilon_{11} \left\{ \left[1 - \left(\frac{z+h/2}{h/2}\right)^2\right] \frac{\partial \Phi}{\partial x} + \frac{z}{h} \frac{\partial V}{\partial x} \right\} \right\}, & -h \leq z \leq 0 \\ (-1)^i \left\{ e_{15} \left(-\psi + \frac{\partial w}{\partial x}\right) + \epsilon_{11} \left\{ \left[1 - \left(\frac{z-h/2}{h/2}\right)^2\right] \frac{\partial \Phi}{\partial x} - \frac{z}{h} \frac{\partial V}{\partial x} \right\} \right\}, & 0 \leq z \leq h \end{cases} \quad (13c)$$

$$D_z = \begin{cases} (-1)^i \left\{ -\left(\bar{e}_{31} - \frac{\bar{c}_{13}}{\bar{c}_{33}}\bar{e}_{33}\right)z \frac{\partial \Psi}{\partial x} + \left(\frac{\bar{e}_{33}^2}{\bar{c}_{33}} + \bar{e}_{33}\right) \left[ 8 \frac{z+h/2}{h^2} \Phi + \frac{1}{h} V \right] \right\}, & -h \leq z \leq 0 \\ (-1)^i \left\{ -\left(\bar{e}_{31} - \frac{\bar{c}_{13}}{\bar{c}_{33}}\bar{e}_{33}\right)z \frac{\partial \Psi}{\partial x} + \left(\frac{\bar{e}_{33}^2}{\bar{c}_{33}} + \bar{e}_{33}\right) \left[ 8 \frac{z-h/2}{h^2} \Phi - \frac{1}{h} V \right] \right\}, & 0 \leq z \leq h \end{cases} \quad (13d)$$

Eq. (13) indicates that there is no fundamental difference between the parallel and series bimorphs under FSDT assumptions since the electromechanical variables are almost the same except for the electric components symmetry.

### 3. Governing equations of motion for the bimorphs

Based on Timoshenko's beam theory and the charge conservation law, the motion equations and the Maxwell's equations of piezoelectric bimorph in Eq. (5) can be satisfied approximately by applying integration over the cross section, namely as

$$\frac{\partial M_x}{\partial x} - Q_x - \int_{-h}^h \rho z \frac{\partial^2 u_x}{\partial t^2} dz = m \quad (14)$$

$$-\frac{\partial Q_x}{\partial x} + \int_{-h}^h \rho \frac{\partial^2 u_z}{\partial t^2} dz = p \quad (15)$$

$$\int_{-h}^0 \left( \frac{\partial D_x}{\partial x} + \frac{\partial D_z}{\partial z} \right) dz = 0 \quad \text{or} \quad \int_0^h \left( \frac{\partial D_x}{\partial x} + \frac{\partial D_z}{\partial z} \right) dz = 0 \quad (16)$$

where  $m$  and  $p$  are the corresponding external couple and force, and  $M$  and  $Q$  are the bending moment and shear force, which can be expressed as:

$$M_x = \int_{-h}^0 z \sigma_x dz + \int_0^h z \sigma_x dz, \quad Q_x = \int_{-h}^0 \tau_{xz} dz + \int_0^h \tau_{xz} dz \quad (17)$$

Eqs. (14), (15) and (16) give the governing equations of piezoelectric bimorphs. For the static case, the governing equations are also valid as long as the time dependent terms such as inertial force and couple are omitted.

As shown in Eq. (10), the defined transverse shear strain merely holds for the value of the midline in each layer, and for explicitness it is notated as  $\gamma_{xz}^m$  (here the superscript  $m$  represents the midline). Thus, to account for the nonlinear distribution of transverse shear stress according to FSDT, the integration of  $\tau_{xz}$  and  $D_x$  over the piezoelectric layer cross-section should be corrected simultaneously by the shear correction factor ( $k$ ) since they both contain the  $\gamma_{xz}^m$  component.

In one piezoelectric layer (e.g. upper layer in parallel case), the shear correction factor,  $k$ , is defined as the ratio of the average shear strain on a section to the value of the midline in each layer, given by

$$k = \frac{\bar{\gamma}_{xz}}{\gamma_{xz}^m} \quad (18)$$

where

$$\bar{\gamma}_{xz} = \frac{1}{h} \int_{-h}^0 \gamma_{xz} dz, \quad \gamma_{xz}^m = -\psi + \frac{\partial w}{\partial x} \quad (19)$$

Substituting the stress components in Eq. (13) into Eq. (17), in view of shear  $k$ , one obtains the expressions for the shear force and moment as

$$Q_x = 2h \left[ c_{55} k \left( -\psi + \frac{\partial w}{\partial x} \right) + e_{15} \left( \frac{2}{3} \frac{\partial \Phi}{\partial x} + \frac{1}{2} \frac{\partial V}{\partial x} \right) \right] \quad (20a)$$

$$M_x = 2h \left[ -\frac{h^2}{3} \left( \bar{c}_{11} - \frac{\bar{c}_{13}^2}{\bar{c}_{33}} \right) \frac{\partial \psi}{\partial x} + \left( \frac{\bar{c}_{13}}{\bar{c}_{33}} \bar{e}_{33} - \bar{e}_{31} \right) \left( \frac{2}{3} \Phi - \frac{1}{2} V \right) \right] \quad (20b)$$

Substituting the electric displacement components in Eq. (13) into Eq. (16) yields

$$\int_{-h}^0 \frac{\partial D_x}{\partial x} dz = e_{15} k \left( -\frac{\partial \psi}{\partial x} + \frac{\partial^2 w}{\partial x^2} \right) h - \varepsilon_{11} \frac{2h}{3} \frac{\partial^2 \Phi}{\partial x^2} - \varepsilon_{11} \frac{h}{2} \frac{\partial^2 V}{\partial x^2} \quad (21a)$$

$$\int_{-h}^0 \frac{\partial D_z}{\partial z} dz = - \left( \bar{e}_{31} - \frac{\bar{c}_{13}}{\bar{c}_{33}} \bar{e}_{33} \right) \frac{\partial \psi}{\partial x} h + \left( \frac{\bar{e}_{13}^2}{\bar{c}_{33}} + \bar{\varepsilon}_{33} \right) \frac{8}{h} \Phi \quad (21b)$$

Substituting Eqs. (9) and (20) into Eqs. (14) and (15), and substituting Eq. (21) into Eq. (16), the governing equations can be rewritten as

$$-b_{11} \frac{\partial w}{\partial x} + \left( b_{21} \frac{\partial^2}{\partial x^2} - b_{12} - b_{41} \frac{\partial^2}{\partial x^2} \right) \psi + (b_{22} - b_{13}) \frac{\partial \Phi}{\partial x} = m + (b_{14} - b_{23}) \frac{\partial V}{\partial x} \quad (22)$$

$$-\left( b_{11} \frac{\partial^2}{\partial x^2} - b_{42} \frac{\partial^2}{\partial x^2} \right) w - b_{12} \frac{\partial \psi}{\partial x} - b_{13} \frac{\partial^2 \Phi}{\partial x^2} = p + b_{14} \frac{\partial^2 V}{\partial x^2} \quad (23)$$

$$b_{31} \frac{\partial^2 w}{\partial x^2} + b_{32} \frac{\partial \psi}{\partial x} + \left( b_{33} \frac{\partial^2}{\partial x^2} + b_{35} \right) \Phi = b_{34} \frac{\partial^2 V}{\partial x^2} \quad (24)$$

where

$$b_{11} = -b_{12} = 2c_{55}hk, \quad b_{13} = \frac{4h}{3}e_{15}, \quad b_{14} = he_{15}, \quad b_{41} = -\frac{2h^3}{3}, \quad b_{42} = 2\rho h \quad (25a)$$

$$b_{21} = -\frac{2h^3}{3} \left( \bar{c}_{11} - \frac{\bar{c}_{13}^2}{\bar{c}_{33}} \right), \quad b_{22} = \frac{4h}{3} \left( \frac{\bar{c}_{13}}{\bar{c}_{33}} \bar{e}_{33} - \bar{e}_{31} \right), \quad b_{23} = -h \left( \frac{\bar{c}_{13}}{\bar{c}_{33}} \bar{e}_{33} - \bar{e}_{31} \right), \quad b_{31} = hke_{15} \quad (25b)$$

$$b_{32} = -h \left[ ke_{15} + \left( \bar{e}_{31} - \frac{\bar{c}_{13}}{\bar{c}_{33}} \bar{e}_{33} \right) \right], \quad b_{33} = -\frac{2h}{3} \varepsilon_{11}, \quad b_{34} = \frac{h}{2} \varepsilon_{11}, \quad b_{35} = \left( \frac{\bar{e}_{13}^2}{\bar{c}_{33}} + \bar{\varepsilon}_{33} \right) \frac{8}{h} \quad (25c)$$

Thus the governing Eqs. (14), (15) and (16) are transformed into (22), (23) and (24) for three independent variables,  $w$ ,  $\psi$  and  $\Phi$  in FSDT beam model. And the shear correction factor,  $k$ , can be calculated numerically according to Eq. (18) from exact 2D solutions under certain loading conditions.

#### 4. Solutions for simply supported bimorph in bending

We consider a piezoelectric bimorph undergoing a surface density of normal force or electric potential applied to the top and bottom faces. Assuming that the shear traction is zero and there is no surface density of moment ( $m=0$ ). The simple support conditions for a beam of length  $l$  are simulated by

$$w|_{x=0,l} = 0, \quad \sigma_x|_{x=0,l} = 0, \quad \phi|_{x=0,l} = 0 \quad (26)$$

The electromechanical load functions are written as Fourier series as follows:

$$p(x,t) = \sum_{n=1}^{\infty} P_n \sin\left(\frac{n\pi}{l}x\right) e^{i\omega t}, \quad V(x,t) = \sum_{n=1}^{\infty} V_n \sin\left(\frac{n\pi}{l}x\right) e^{i\omega t} \quad (27)$$

where for uniform distribution case, we have

$$P_n = \frac{2P_0}{n\pi} [1 - (-1)^n], \quad V_n = \frac{2V_0}{n\pi} [1 - (-1)^n] \quad (28)$$

A solution to the set of linear equations which satisfies the boundary conditions for bending of a simply supported beam can be searched for as Fourier series

$$w(x,t) = \sum_{n=1}^{\infty} W_n \sin\left(\frac{n\pi}{l}x\right) e^{i\omega t} \quad (29a)$$

$$\psi(x,t) = \sum_{n=1}^{\infty} \Psi_n \cos\left(\frac{n\pi}{l}x\right) e^{i\omega t} \quad (29b)$$

$$\Phi(x,t) = \sum_{n=1}^{\infty} \Phi_n \sin\left(\frac{n\pi}{l}x\right) e^{i\omega t} \quad (29c)$$

Substituting Eqs. (27) and (29) into (22), (23) and (24), and the results expressed in matrix form are:

$$\begin{bmatrix} a_{11} & a_{12} & a_{13} \\ a_{21} & a_{22} & a_{23} \\ a_{31} & a_{32} & a_{33} \end{bmatrix} \begin{Bmatrix} W_n \\ \Psi_n \\ \Phi_n \end{Bmatrix} = \begin{Bmatrix} a_{14} V_n \\ P_n + a_{24} V_n \\ a_{34} V_n \end{Bmatrix} \quad (30)$$

where

$$a_{11} = b_{11} \frac{n\pi}{l}, \quad a_{12} = -b_{21} \left(\frac{n\pi}{l}\right)^2 - b_{12} + b_{41} \omega_n^2, \quad a_{13} = (b_{22} - b_{31}) \frac{n\pi}{l}, \quad a_{14} = (b_{14} - b_{23}) \frac{n\pi}{l} \quad (31a)$$

$$a_{21} = b_{11} \left(\frac{n\pi}{l}\right)^2 - b_{42} \omega_n^2, \quad a_{22} = b_{12} \frac{n\pi}{l}, \quad a_{23} = b_{13} \left(\frac{n\pi}{l}\right)^2, \quad a_{24} = -b_{14} \left(\frac{n\pi}{l}\right)^2 \quad (31b)$$

$$a_{31} = -b_{31} \left(\frac{n\pi}{l}\right)^2, \quad a_{32} = -b_{32} \frac{n\pi}{l}, \quad a_{33} = -b_{33} \left(\frac{n\pi}{l}\right)^2 + b_{35}, \quad a_{34} = -b_{34} \left(\frac{n\pi}{l}\right)^2 \quad (31c)$$

Solving Eq. (30) for  $W_n$ ,  $\Psi_n$  and  $\Phi_n$  give the Fourier coefficients in Eq. (29), based on which other

relative electromechanical variables are readily obtained.

## 5. Numerical results and analysis

The geometry of the bimorph is  $l = 1$  m with different length-to-thickness ratios  $l/(2h)$  considered. The piezoelectric layer material used for the numerical investigation is PZT-5A, and the material properties are listed in Table 1. Two kinds of electromechanical loads are considered corresponding to (1) sensor function with a force density per unit area applied to the upper face of the bimorph in closed circuit and (2) actuator function with an electric potential applied to the top and bottom faces of the bimorph. The numerical results for state variables are given in dimensionless units as follows (Fernandes and Pouget 2003).

(1) For surface force density  $P_0 \neq 0$  ( $P_0 = 1000$  N/m<sup>2</sup> and  $V_0 = 0$ ), we define

$$(U, W, \Phi) = \frac{\bar{c}_{11}}{hP_0}(u, w, \phi/E_0), \quad (T_{ij}, D_k) = \frac{1}{P_0}(\sigma_{ij}, E_0 D_k) \quad (32)$$

(2) For electric potential  $V_0 \neq 0$  ( $V_0 = 1000$  V and  $P_0 = 0$ ), we define

$$(U, W, \Phi) = \frac{E_0}{V_0}(u, w, \phi/E_0), \quad (T_{ij}, D_k) = \frac{hE_0}{\bar{c}_{11}V_0}(\sigma_{ij}, E_0 D_k) \quad (33)$$

For numerical convenience we take  $E_0 = 10^{10}$  V/m. The series terms number of Eqs. (27) and (29) are adjusted in order to satisfy the convergence. The 2D benchmark computations for comparison are performed via state space approach.

The calculated and adopted shear correction factor ( $k$ ) for different length-to-thickness ratios are given in Table 2. For the condition of static force density uniformly applied on the top face of the bimorph, the calculated  $k$  is found to be very close to the Timoshenko (1922) recommended value 8/9 for plane stress problem; while for the condition of electric potential applied to surface electrodes,  $k$  is slightly higher and found to change somewhat irregularly for different aspect ratios but is within the range of 0.9-1.0. Thus, for the explicitness and ease of use, we propose  $k = 8/9$  for bimorphs under plane stress assumption despite the different load conditions.

### 5.1. Applied surface density of normal force (sensor function)

For this case the applied electrical potential is set to zero and a uniform surface density of normal

Table 1 Independent constants of piezoelectric material (PZT-5A)

$\rho$	$c_{11}$	$c_{12}$	$c_{33}$	$c_{13}$	$c_{55}$	$e_{31}$	$e_{33}$	$e_{15}$	$\varepsilon_{11}$	$\varepsilon_{33}$
7800	105	54.6	86.8	52.7	22.2	-9.78	13.8	12.2	16.4	15.1

Unit:  $\rho$ -kg/m<sup>3</sup>,  $c$ - $10^9 \times$  N/m<sup>2</sup>,  $e$ -C/m<sup>2</sup>,  $\varepsilon$ - $10^{-9} \times$  C/Vm

Table 2 Calculated and adopted  $k$  values for different length-to-thickness ratios

Load type	$l/2h$	100	50	20	10	5
Force density	Calculated	0.8887	0.8887	0.8886	0.8886	0.8887
	Adopted	8/9	8/9	8/9	8/9	8/9
Electric potential	Calculated	0.9449	0.9368	0.9209	0.9588	0.9725
	Adopted	8/9	8/9	8/9	8/9	8/9

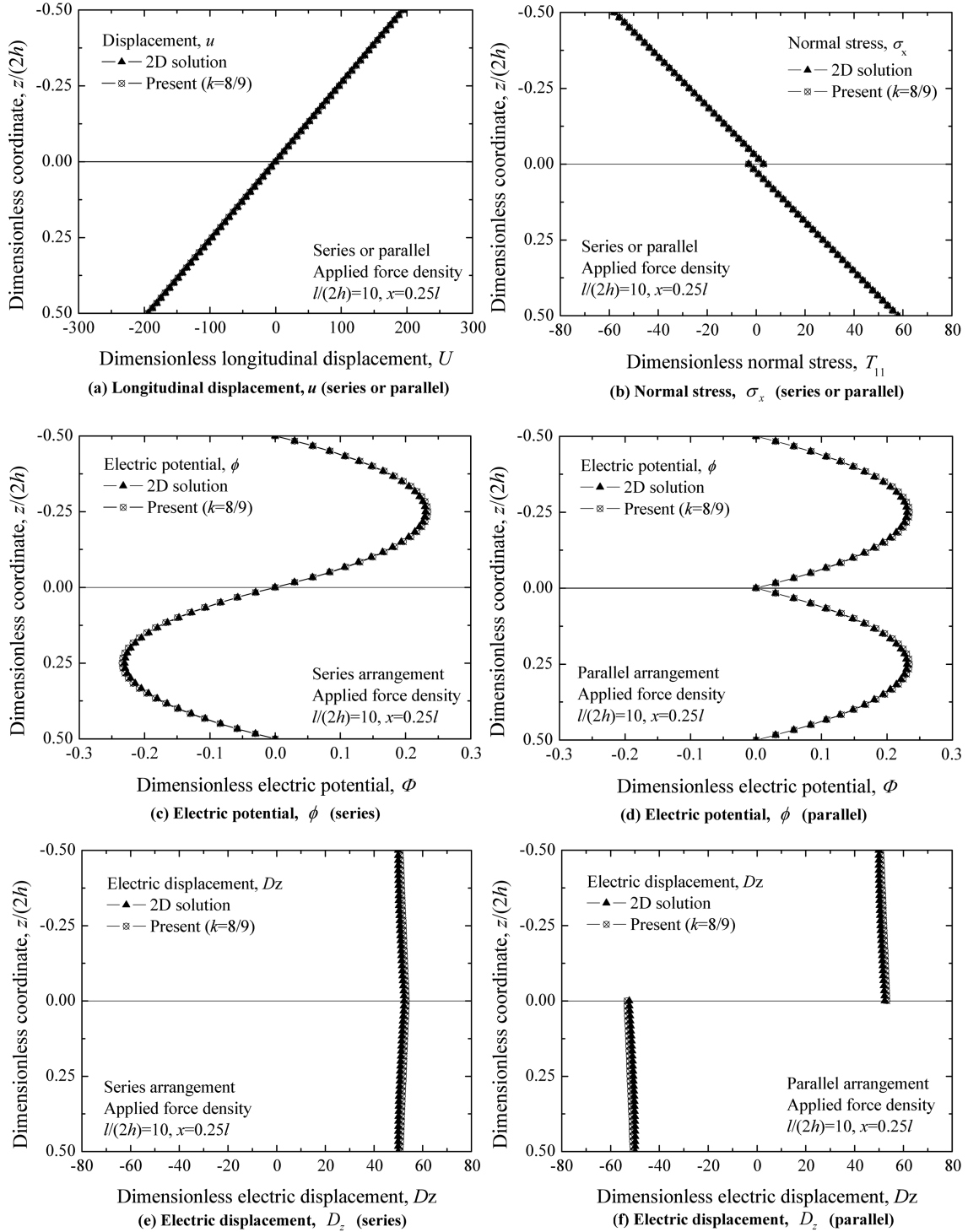


Fig. 3 Local responses under applied force density,  $l/(2h) = 10$

Table 3 Typical static responses, applied uniform force density

$l/(2h)$	Methods	$W$ ( $l/4, 0$ )	Error (%)	$T_{11}$ ( $l/4, 0$ )	Error (%)	$\Phi$ ( $l/4, h/2$ )	Error (%)
50	2D solution	786895		1444		1.145	
	Present ( $k=8/9$ )	786915	0	1444	-0.01	1.145	0.06
	Present ( $k=5/6$ )	786974	0.01	1444	-0.01	1.145	0.06
10	2D solution	1292		57.98		0.2306	
	Present ( $k=8/9$ )	1292	0.06	57.78	-0.34	0.2342	1.57
	Present ( $k=5/6$ )	1295	0.25	57.78	-0.34	0.2342	1.57
5	2D solution	87.02		14.67		0.1179	
	Present ( $k=8/9$ )	87.26	0.28	14.47	-1.38	0.1251	6.15
	Present ( $k=5/6$ )	87.85	0.95	14.47	-1.38	0.1251	6.15

force ( $P_0 = 1000 \text{ N/m}^2$ ) is applied to the top face of the bimorphs. Then in present approach, the  $V_n$  in the right-hand side and the frequency related terms in the coefficients matrix of Eq. (30) should be omitted. The numerical results of static responses at the position  $x=0.25l$  for typical length-to-thickness ratio  $l/(2h)=10$  are illustrated in Fig. 3(a)-(f), and the estimating errors between the present model and 2D solution for  $l/(2h)=50, 10$ , and  $5$  are selected and given in Table 3.

As shown in Fig. 3, the elongation displacement  $u$ , normal stress  $\sigma_x$ , induced electric potential  $\phi$  and electric displacement  $D_z$  in present model agree well with those of 2D solutions. In Fig. 3(c) the induced electric potential is antisymmetric about the neutral axis of the bimorph for series arrangement, and the continuity condition for  $D_z$  is then satisfied as shown in Fig. 3(e). In Fig. 3(d) we have the induced electric potential showing a symmetric profile for parallel arrangement, and this explains the jump in the electric induction as shown in Fig. 3(f). As shown in Table 3, even for thick bimorph  $l/(2h)=5$ , the discrepancy of the deflection  $w$  dose not exceed 1%. The most interesting result in Table 3 is that the errors of the static local responses predicted by present model with either  $k=8/9$  or  $k=5/6$  (Cowper 1966) are almost the same, except for the transverse displacement  $w$ .

## 5.2. Applied electric potential (actuator function)

In this situation, the piezoelectric bimorph suffers an electric potential ( $V_0 = 1000 \text{ V}$ ) applied to the top and bottom faces ( $+V_0$  at  $z=-h$  and  $-V_0$  at  $z=h$  for series case, and  $+V_0$  at both surfaces for parallel case, with  $P_0=0$ ). Then  $P_n$  in the right-hand side of Eq. (30) should be set to zero and the frequency related terms in the coefficients matrix are omitted. The numerical results are plotted in Fig. 4(a)-(f) and the estimating errors are given in Table 4.

As shown in Fig. 4, although the local responses of the electromechanical variables are basically different from those in the case of applied force density (especially for  $\phi$ ), the accuracy predicted by the present model is warranted again. The linear variation through the thickness with  $u$  in Fig. 4(a) indicates that the bimorph also undergoes a bending motion. However, compared with the performance of sensor function listed in Table 3, the discrepancy of predictions in Table 4 is slightly larger, which indicates that the present model will perform differently from the sensor to actuator functions.

It can be readily concluded from Table 3 and Table 4 that, in static response analyses, the shear correction factor influences the behaviors of FSDT solution little except for the transverse displacement  $w$ . The interesting finding echoes what Timoshenko stated about the shear deformation effect on the

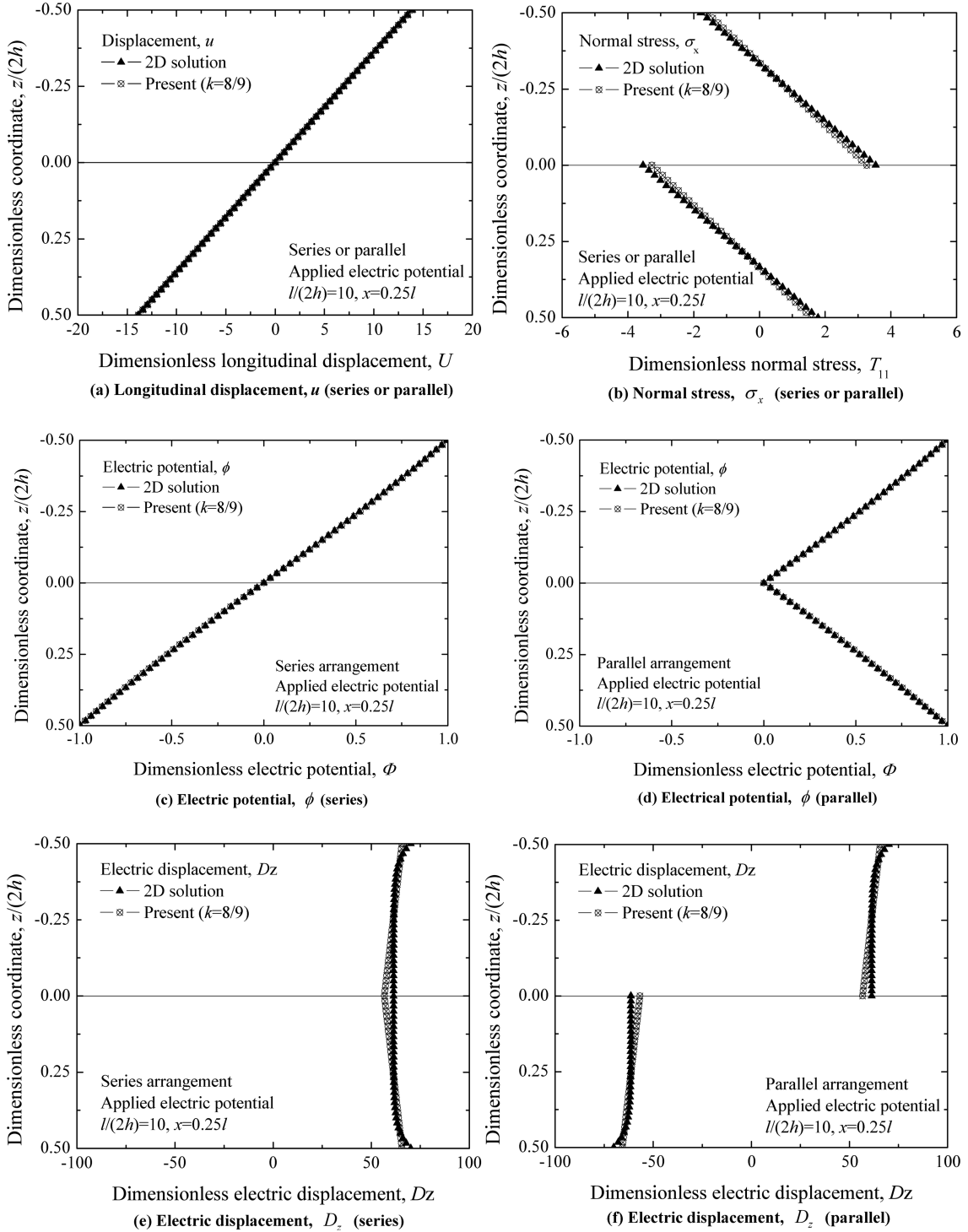


Fig. 4 Local responses under applied electric potential,  $l/(2h) = 10$

Table 4 Typical static responses, applied electric potential

$l/(2h)$	Methods	$W$ ( $l/4, 0$ )	Error (%)	$T_{11}$ ( $l/4, 0$ )	Error (%)	$\Phi$ ( $l/4, h/2$ )	Error (%)
50	2D solution	2602		3.535		0.5200	
	Present ( $k=8/9$ )	2607	0.22	3.315	-6.22	0.5253	1.02
	Present ( $k=5/6$ )	2608	0.25	3.315	-6.22	0.5253	1.02
10	2D solution	103.4		3.538		0.5200	
	Present ( $k=8/9$ )	106.3	2.75	3.298	-6.78	0.5255	1.06
	Present ( $k=5/6$ )	109.8	6.18	3.298	-6.78	0.5255	1.06
5	2D solution	25.31		3.538		0.5200	
	Present ( $k=8/9$ )	27.50	8.64	3.285	-7.14	0.5260	1.22
	Present ( $k=5/6$ )	30.73	21.38	3.285	-7.14	0.5260	1.22

static deflection problems (Gere and Timoshenko 1984).

### 5.3. Free vibration analysis of piezoelectric bimorphs

In this section, we propose the prediction of modal frequencies of the bimorphs for both closed circuit ( $\phi = 0$  at outer surfaces) and open circuit ( $D_z = 0$  at outer surfaces) conditions on surfaces of the bimorph, for different length-to-thickness ratios  $l/(2h)=100, 50, 20, 10$  and  $5$ . For closed circuit condition, the right-hand side of Eq. (30) is directly set to zero, and nontrivial solutions for  $W_n, \Psi_n$  and  $\Phi_n$  implies that the determinant of the coefficients matrix of Eq. (30) vanishes. Then solving Eq. (30) gives the frequencies of flexural vibrations for a given  $n$ . For open circuit condition, there is non-zero but uniform distribution of electric potential in the outer electrodes, thus the  $V_n$  in the right-hand side of Eq. (30) become an unknown variable. Eq. (30) should be readily reconstructed in view of the boundary condition ( $D_z = 0$  at outer surfaces) and the consequent coefficient matrix is  $4 \times 4$  now. Then the modal frequencies are obtained similarly. The dimensionless modal frequency is  $\Omega = (2h)\omega\sqrt{\rho/\bar{c}_{11}}$ .

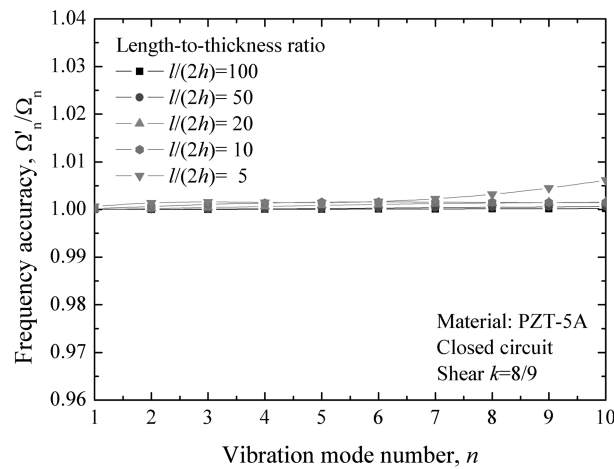
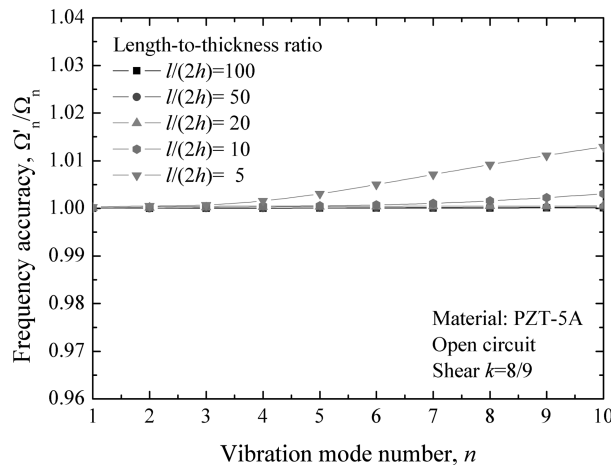


Fig. 5 Modal frequency accuracy ( $k = 8/9$ , closed circuit)

Table 5 Modal frequency performance in closed circuit ( $l/2h=10$ )

Vibration modes	2D solution	Present ( $k=8/9$ )	Error (%)	Present ( $k=5/6$ )	Error (%)	Present ( $k=\pi^2/12$ )	Error (%)
$n=1$	0.2634	0.2635	0.02	0.2633	-0.07	0.2632	-0.09
$n=2$	1.005	1.005	0.06	1.002	-0.25	1.002	-0.32
$n=3$	2.113	2.115	0.11	2.103	-0.49	2.100	-0.62
$n=4$	3.474	3.478	0.14	3.448	-0.75	3.441	-0.93
$n=5$	5.000	5.008	0.15	4.951	-1.00	4.939	-1.24
$n=6$	6.635	6.646	0.16	6.554	-1.23	6.535	-1.52
$n=7$	8.341	8.354	0.15	8.221	-1.44	8.194	-1.76
$n=8$	10.10	10.11	0.15	9.932	-1.62	9.896	-1.98
$n=9$	11.88	11.90	0.14	11.67	-1.77	11.63	-2.17
$n=10$	13.70	13.72	0.14	13.44	-1.90	13.38	-2.32

Fig. 6 Modal frequency accuracy ( $k=8/9$ , open circuit)

For closed circuit case, the accuracy performance of the modal frequencies predicted by the present model with  $k=8/9$  are shown in Fig. 5, and the detailed results of  $l/(2h)=10$  is presented in Table 5, with  $k=8/9$ ,  $k=5/6$  and  $k=\pi^2/12$  (Mindlin 1951). It is clear that rather good agreement is observed for the present model. For open circuit case as shown in Fig. 6 and Table 6, although the frequency values are slightly higher than those in closed circuit case for a given  $n$ , the prediction performance is similarly fine. Nevertheless, the difference among the results using different  $k$  values implies that the dynamic prediction based on FSDT is sensitive to the exactness of shear  $k$ .

## 6. Summary and conclusions

In the present study, the piezoelectric bimorph structure has been investigated in detail statically and

Table 6 Modal frequency performance in open circuit ( $l/2h=10$ )

Vibration modes	2D solution	Present ( $k=8/9$ )	Error (%)	Present ( $k=5/6$ )	Error (%)	Present ( $k=\pi^2/12$ )	Error (%)
$n=1$	0.2730	0.2730	0.01	0.2727	-0.10	0.2726	-0.11
$n=2$	1.033	1.034	0.03	1.030	-0.35	1.029	-0.40
$n=3$	2.154	2.155	0.04	2.141	-0.66	2.138	-0.75
$n=4$	3.515	3.516	0.05	3.483	-0.95	3.476	-1.10
$n=5$	5.031	5.034	0.05	4.973	-1.21	4.960	-1.40
$n=6$	6.652	6.656	0.07	6.562	-1.42	6.542	-1.65
$n=7$	8.346	8.355	0.10	8.221	-1.60	8.193	-1.83
$n=8$	10.10	10.11	0.16	9.934	-1.76	9.897	-1.96
$n=9$	11.89	11.91	0.22	11.69	-1.88	11.64	-2.05
$n=10$	13.71	13.75	0.31	13.48	-1.99	13.42	-2.10

dynamically (free vibration) based on improved FSDT approach. From the analytical modelling and numerical analysis, it was found that:

- (1) Piezoelectric bimorphs will behave fundamentally the same for series and parallel arrangements under the same loading conditions except for the symmetry of electric variables. While for a certain arrangement, the detailed distributions of electromechanical variables for the case of being applied force density differ from those of being applied electric potential, which reflects the sensor and actuator behaviors of piezoelectric bimorphs.
- (2) In both static and dynamic analysis, the present model obtains very accurate prediction with the proposed shear correction factor,  $k=8/9$ . The static response investigation indicates that the present model performs slightly better for the sensor function than for the actuator function. High accuracy of modal frequencies is acquired even for rather thick beam, whereas classical beam or plate theory gives less accurate results.
- (3) In FSDT model, shear correction factor plays a key role in assuring the prediction accuracy of dynamic response while influence the static results little. Thus, it is very important to choose the appropriate  $k$  value in dynamic problems when using FSDT approaches, especially for the vibration control applications in smart structures and systems.

## Acknowledgements

This work was supported by the research grants from National Natural Science Foundation of China (No. 10472102 and No. 10372089). And the helpful advice on this study from Prof. Wei-qiu Chen and Dr. Hui-ming Wang of Zhejiang University are greatly appreciated. The authors also wish to thank the editor, Prof. Jan-ming Ko of Hong Kong Polytechnic University and the anonymous reviewers whose valuable comments led to substantial improvement of this paper.

## References

- Chee, C. Y. K., Tong, L. and Steven, G. P. (1998), "A review on the modelling of piezoelectric sensors and actuators incorporated in intelligent structures", *J. Intell. Mater. Syst. Struct.*, **9**(1), 3-19.
- Cowper, G. R. (1966), "The shear coefficient in Timoshenko's beam theory", *J. Appl. Mech.*, ASME, **33**(2), 335-340.
- Ding, H. J., Wang, G. Q. and Chen, W. Q. (1997), "Green's functions for a two-phase infinite piezoelectric plane", *Proc. of Royal Society of London (A)*, **453**(1966/8), 2241-2257.
- Ding, H. J., Chen, W. Q. and Xu, R. Q. (2000), "New state space formulations for transversely isotropic piezoelectricity with application", *Mech. Res. Commun.*, **27**(3), 319-326.
- Fernandes, A. and Pouget, J. (2003), "Analytical and numerical approaches to piezoelectric bimorph", *Int. J. Solids Struct.*, **40**(17), 4331-4352.
- Gere, J. M. and Timoshenko, S. P. (1984), *Mechanics of Materials*, 2<sup>nd</sup> Ed., PWS-KENT Publishing Company, Boston.
- Gopinathan, S.V., Varadan, V.V. and Varadan, V.K. (2000), "A review and critique of theories for piezoelectric laminates", *Smart Mater. Struct.*, **9**(1), 24-48.
- Ha, S. K. and Kim, Y. H. (2002), "Analysis of a piezoelectric multi-morph in extentional and flexural motions", *J. Sound Vib.*, **253**(5), 1001-1014.
- He, L.-H., Lim, C. W. and Soh, A. K. (2000), "Three-dimensional analysis of an antiparallel piezoelectric bimorph", *Acta Mech.*, **145**(1-4), 189-204.
- Hwang, W. S. and Park, H. C. (1993), "Finite element modeling of piezoelectric sensors and actuators", *AIAA J.*, **31**(5), 930-937.
- Kapurja, S. (2001), "An efficient coupled theory for multilayered beams with embedded piezoelectric sensory and active layers", *Int. J. Solids Struct.*, **38** (50-51), 9179-9199.
- Lee, J. S. and Jiang, L. Z. (1996), "Exact electroelastic analysis of piezoelectric laminae via state space approach", *Int. J. Solids Struct.*, **33**(7), 977-990.
- Lim, C. W., He, L.-H. and Soh, A. K. (2001), "Three-dimensional electromechanical responses of a parallel piezoelectric bimorph", *Int. J. Solids Struct.*, **38**(16), 2833-2849.
- Mindlin, R. D. (1951), "Influence of rotary inertia and shear on flexural motions of isotropic, elastic plates", *J. Appl. Mech.*, **18**(1), 31-38.
- Rao, S. S. and Sunar, M. (1994), "Piezoelectricity and its use in disturbance sensing and control of flexible structures: a survey", *Appl. Mech. Rev.*, ASME, **47**(4), 113-123.
- Saravanos, D. A. and Heyliger, P. R. (1999), "Mechanics and computational models for laminated piezoelectric beams, plates and shells", *Appl. Mech. Rev.*, ASME, **52**(10), 305-320.
- Smits, J. G., Dalke, S. I. and Cooney, T. K. (1991), "The constituent equations of piezoelectric bimorphs", *Sens. Actuators A Phys.*, **28**(1), 41-61.
- Sosa, H. A. and Castro, M. A. (1993), "Electroelastic analysis of piezoelectric laminated structures", *Appl. Mech. Rev.*, ASME, **46**(11/2), 21-28.
- Steel, M. R., Harrison, F. and Harper, P. G. (1978), "The piezoelectric bimorph: an experimental and theoretical study of its quasistatic response", *J. Phys. D.*, **11**(6), 979-989.
- Tarn, J. Q. (2002), "A state space formalism for piezothermoelasticity", *Int. J. Solids Struct.*, **39**(20), 5173-5184.
- Timoshenko, S. P. (1922), "On the transverse vibrations of bars of uniform cross section", *Phil. Mag.*, **43**(6), 125-131.
- Tzou, H. S. and Tiersten, H. F. (1994), "Elastic analysis of laminated composite plates in cylindrical bending due to piezoelectric actuators", *Smart Mater. Struct.*, **3**(3), 255-265.
- Wang, Q. and Quek, S. T. (2000), "Flexural vibration analysis of sandwich beam coupled with piezoelectric actuator", *Smart Mater. Struct.*, **9**(1), 103-109.
- Wang, S. Y. (2004), "A finite element model for the static and dynamic analysis of a piezoelectric bimorph", *Int. J. Solids Struct.*, **41**(15), 4075-4096.
- Zhou, Y. G. and Chen, Y. M. (2005), "Influence of seismic cyclic loading history on small strain shear modulus of saturated sands", *Soil Dyn. Earthq. Eng.*, **25**(5), 341-353.